

Electronic Supplementary Information

Organic conducting wire formation on a TiO₂ nanocrystalline structure: towards
long-lived charge separated systems

Yasuhiro Tachibana, Satoshi Makuta, Yasuhide Otsuka, Jun Terao,† Susumu Tsuda,*

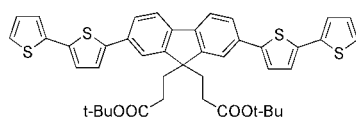
Nobuaki Kambe, Shu Seki and Susumu Kuwabata

Department of Applied Chemistry, Graduate School of Engineering, Osaka University,
Yamada-oka, Suita, Osaka 565-0871, Japan. *Email: y.tachibana@chem.eng.osaka-u.ac.jp,
Tel&Fax: +81-(0) 6-6879-7374, †Current address: Department of Energy and Hydrocarbon
Chemistry, Graduate School of Engineering, Kyoto University, Katsura, Nishikyo-ku, Kyoto,
615-8510

1. Monomer synthesis

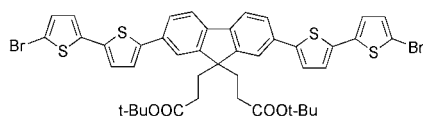
2,7-diiodofluorene-9,9-dipropionic acid di-tert-butyl ester was prepared by the procedure reported previously by J. J. Michels *et al.*¹ Other reagents were purchased from commercial sources and used without further purification. Melting points were measured with a Stanford Research Systems MPA100 apparatus. Matrix assisted laser desorption/ionization time-of-flight (MALDI-TOF) mass spectra were obtained with dithranol as a matrix on a SHIMADZU KRATOS TOF MASS spectrometer AXIMA-CFR Plus. ¹H NMR for 400 MHz and ¹³C NMR for 100MHz spectra were recorded by a JEOL JNM-Alice 400 spectrometer. High-resolution mass spectra were determined on a JMS-T100TD spectrometer. Elemental analyses were performed on Perkin Elmer 240C apparatus in the Instrumental Analysis Center of the Faculty of Engineering, Osaka University.

Synthesis of 2,7-bis(bithiophene)fluorene-9,9-dipropionic acid di-tert-butyl ester



To a mixture of 2,7-diiodofluorene-9,9-dipropionic acid di-tert-butyl ester (1.1 g, 1.6 mmol), 2,2'-bithiophene-5-boronic acid pinacol ester (1.0 g, 3.4 mmol), Na₂CO₃ (1.7 g, 16 mmol), and Pd(PPh₃)₄ (370 mg, 0.32 mmol) in THF (10 mL) was added dimethoxyethane (20 mL) and H₂O (5 mL) under a nitrogen atmosphere. After stirring for 15 h at 80 °C and cooling to room temperature, the reaction mixture was extracted with EtOAc. The organic layer was washed with brine, dried over Na₂SO₄, the solvent was removed *in vacuo*, and the residue was purified by column chromatography on silica gel (10% EtOAc in hexane) to yield 2,7-bis(bithiophene)fluorene-9,9-dipropionic acid di-*tert*-butyl ester as a yellow solid (690 mg, 58%). m.p.: 192-193 °C; MALDI-TOF MS: (*m/z*) 751 [M]⁺ (calcd: 751); ¹H NMR (400MHz, CD₂Cl₂, 21.0 °C): δ_H = 7.72 (d, *J* = 7.8 Hz, 2H), 7.64-7.61 (m, 4H), 7.34 (d, *J* = 3.9 Hz, 2H), 7.26-7.23 (m, 4H), 7.19 (d, *J* = 3.7 Hz, 2H), 7.04 (dd, *J* = 3.7, 5.1 Hz, 2H), 2.40 (t, 4H), 1.51 (t, 4H), 1.25 (s, 18H); ¹³C NMR (400 MHz, CD₂Cl₂, 20.2 °C): δ_C = 172.7, 149.7, 143.6, 140.6, 137.7, 137.0, 133.8, 128.3, 125.6, 125.0, 124.9, 124.3, 124.0, 120.9, 120.3, 80.2, 54.2, 34.9, 30.3, 28.0; Anal. Calcd for C₄₃H₄₂O₄S₄: C, 68.76; H, 5.64%; Found: C, 68.48; H, 5.43%

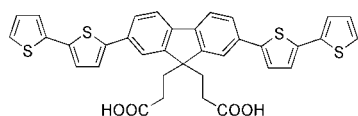
Synthesis of 2,7-bis(2-bromobithiophene)fluorene-9,9'-dipropionic acid di-tert-butyl ester



To a mixture of 2,7-bis(bithiophene)fluorene-9,9'-dipropionic acid di-tert-butyl ester (260 mg,

0.35 mmol) in DMF (15 mL) at 0 °C was added NBS (137 mg, 0.77 mmol). The mixture was stirred at room temperature for 7 h. The reaction mixture was extracted with EtOAc. The organic layer was washed with brine, dried over Na₂SO₄, the solvent was removed *in vacuo*, and the residue was purified by column chromatography on silica gel (20% EtOAc in hexane) to yield 2,7-bis(2-bromobithiophene)fluorene-9,9'-dipropionic acid di-*tert*-butyl ester as a yellow solid (270 mg, 86%). m.p.: 184-187 °C; ¹H NMR (400MHz, CD₂Cl₂, 19.8 °C): δ_H = 7.72 (d, *J* = 8.5 Hz, 2H), 7.63-7.60 (m, 4H), 7.33 (d, *J* = 3.7 Hz, 2H), 7.13 (d, *J* = 3.7 Hz, 2H), 7.01 (d, *J* = 3.7 Hz, 2H), 6.98 (d, *J* = 3.7 Hz, 2H), 2.40 (t, 4H), 1.50 (t, 4H), 1.24 (s, 18H); ¹³C NMR (400 MHz, CD₂Cl₂, 19.9 °C): δ_C = 172.6, 149.8, 144.1, 140.8, 139.3, 135.8, 133.6, 131.3, 125.7, 125.4, 124.4, 124.2, 120.9, 120.4, 111.2, 80.2, 54.2, 34.9, 30.3, 28.0; HRMS Calcd for C₄₃H₄₀Br₂O₄S₄·Na: 929.0074; Found: 929.0068.

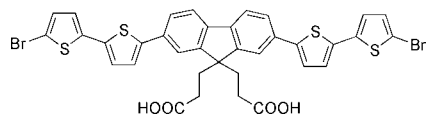
Synthesis of 2,7-bis(bithiophene)fluorene-9,9-dipropionic acid (F1BT2H)



Trifluoroacetic acid (TFA) (2 mL) was added to a solution of 2,7-bis(bithiophene)fluorene-9,9-dipropionic acid di-*tert*-butyl ester (56 mg, 0.075 mmol) in CH₂Cl₂ (3 mL) at 0 °C. The mixture was stirred for 10 h at room temperature. The solvents were evaporated under reduced pressure. Residues of TFA were removed by repeated addition and evaporation of small aliquots of toluene and the residue was purified by column chromatography on silica gel (diethylether) to yield 2,7-bis(bithiophene)fluorene-9,9-dipropionic acid as a yellow solid (23 mg, 48%). m.p.: 240-243 °C ; MALDI-TOF MS: (*m/z*) 638 [M]⁺ (calcd: 639); ¹H NMR (400MHz, DMSO-*d*₆, 28.4 °C): δ_H = 11.84 (bs, 2H, COOH), 7.90 (d, *J* = 8.2 Hz, 2H), 7.86 (s, 2H), 7.71 (d, *J* = 8.2

Hz, 2H), 7.63 (d, $J = 3.6$ Hz, 2H), 7.54 (d, $J = 5.1$ Hz, 2H), 7.39 (d, $J = 3.4$ Hz, 2H), 7.36 (d, $J = 3.6$ Hz, 2H), 7.13 (dd, $J = 3.4$ 5.1 Hz, 2H), 2.44(t, 4H) , 1.44 (t, 4H); ^{13}C NMR (400 MHz, DMSO- d_6 , 28.4 °C): $\delta_{\text{C}} = 173.8, 149.3, 142.3, 139.7, 136.3, 135.7, 132.7, 128.4, 125.4, 125.0, 124.94, 124.86, 124.0, 120.8, 119.7, 53.6, 33.6, 28.8$; Anal. Calcd for $\text{C}_{35}\text{H}_{26}\text{O}_4\text{S}_4$: C, 65.80; H, 4.10%; Found: C, 65.52; H, 4.48%

Synthesis of 2,7-bis(2-bromobithiophene)fluorene-9,9'-dipropionic acid (F1BT2Br)



Trifluoroacetic acid (TFA) (2 mL) was added to a solution of 2,7-bis(2-bromobithiophene)fluorene-9,9-dipropionic acid di-tert-butyl ester (50 mg, 0.055 mmol) in CH_2Cl_2 (2 mL) at 0 °C. The mixture was stirred for 2 h at room temperature. The solvents were evaporated under reduced pressure. Residues of TFA were removed by repeated addition and evaporation of small aliquots of toluene and the residue was purified by column chromatography on silica gel (diethylether) to yield 2,7-bis(2-bromobithiophene)fluorene-9,9-dipropionic acid as a yellow solid (20 mg, 46%). m.p.: 243-245 °C; ^1H NMR (400MHz, DMSO- d_6 , 28.4 °C): $\delta_{\text{H}} = 11.85$ (bs, 2H, COOH), 7.89 (d, $J = 8.3$ Hz, 2H), 7.85 (s, 2H), 7.68 (d, $J = 8.3$ Hz, 2H), 7.62 (d, $J = 3.8$ Hz, 2H), 7.36 (d, $J = 3.8$ Hz, 2H), 7.24 (d, $J = 3.8$ Hz, 2H), 7.21 (d, $J = 3.8$ Hz, 2H), 2.42(t, 4H) , 1.42 (t, 4H); ^{13}C NMR (400 MHz, DMSO- d_6 , 28.4 °C): $\delta_{\text{C}} = 173.7, 149.3, 143.0, 139.8, 138.1, 134.3, 132.5, 131.6, 125.7, 125.03, 125.97, 124.5, 120.9, 119.8, 110.1, 53.7, 33.6, 28.8$; HRMS Calcd for $\text{C}_{35}\text{H}_{23}\text{Br}_2\text{O}_4\text{S}_4$: 792.8846; Found: 792.8852.

2. Experimental

Preparation of nanocrystalline metal oxide film and conducting wire formation

Anatase TiO₂ nanocrystalline films, thickness 6~7 μm, were prepared on a slide glass or a fluorine doped tin oxide glass, FTO, (Asahi glass, type-U, 10 Ω/square) by a screen printer. The TiO₂ paste, Ti-Nanoxide (particle diameter of approximately 15 nm), were purchased from Solaronix SA. The film, after printing, was leveled for 15 min, heated up to 500 °C at 15.8 °C/min, and calcined at 500 °C for 1 h in an air flow oven. Al₂O₃ nanoporous films, thickness: 7 μm, were prepared using Degussa Aluminum Oxide (Alu C, γ-Al₂O₃: 67%, δ-Al₂O₃: 33%, tetragonal crystal system, particle diameter of approximately 13 nm) by the previously reported methods.² The printed Al₂O₃ films were calcined at 500 °C for 1 h in air. Attachment of F1BT2R on the TiO₂ or Al₂O₃ surface was performed by dipping a film in 50 μM F1BT2R dissolved in ethanol or tetrahydrofuran (THF) at room temperature overnight. The F1BT2R adsorbed metal oxide film was thoroughly washed by ethanol to remove any F1BT2R that did not attach to the metal oxide surface.

Conducting wire formation was achieved by applying an electrical bias to F1BT2H (α-terminal atom is H) adsorbed TiO₂ or Al₂O₃ electrode, typically at 1.0 V vs. Ag/AgCl, in the electrolyte containing 0.1 M lithium perchlorate, LiClO₄, (Wako) in propylene carbonate, PC, (Wako) in a three-electrode cell. The polymerization apparently proceeds initially by oxidizing the attached F1BT2H adjacent to the FTO surface, and then the oxidized bithiophene terminal of one molecule reacts with the bithiophene terminal of the other molecule, forming a quarter-thiophene unit as a result of α-α' coupling. The formed oligomer is oxidized again, and the neighboring F1BT2H is in turn oxidized by this oxidized oligomer, increasing the conducting wire length. This polymerization scheme is similar to polythiophene formation.³ After the polymerization, the hybrid film, P-F1BT2/TiO₂, was thoroughly washed with ethanol and dried in air.

As a control sample, the P-F1BT2 was also prepared by electrochemical polymerization of the F1BT2H, directly on FTO after the clean FTO was placed in a three-electrode cell, containing 50 μM F1BT2H and 0.1 M LiClO_4 in acetonitrile. The polymerization was performed by applying +1.0 V vs Ag/AgCl to the FTO support. The onset oxidation potential was confirmed to be +0.8 V vs. Ag/AgCl, when a Pt electrode was employed as a working electrode in a three-electrode cell.

AFM measurements

The film surface morphology was observed by an atomic force microscopy, AFM (SPI-4000, SEIKO Instruments Inc.).⁴ The tapping mode was used to obtain topographic and phase images simultaneously with a resonance frequency of approximately 170 kHz and a scan rate of 1 Hz. For all samples, almost identical mean tip-to-sample distance was employed to achieve direct comparison of material dependent phase contrast.⁵ The contrast, i.e. phase shift, of the images was normalized to achieve direct comparison of difference in energy dissipation from the tip-sample interaction between samples.⁶

Optical measurements

Absorption and emission spectra were measured by a UV/Vis absorption spectrometer (JASCO, V-670) and an emission spectrometer (Horiba, FluoroLog-3), respectively. IR spectra were measured by FT-IR spectrometer with an ATR arrangement (Perkin Elmer, Spectrum 100), with the data collection at a resolution of 1 cm^{-1} .

Adsorption isotherm studies were conducted by estimating F1BT2H adsorption amount on the TiO_2 surface. The TiO_2 film was immersed in 10 mL F1BT2H ethanol solution of predetermined concentration for 20 hours at room temperature. The film was subsequently removed, rinsed thoroughly with ethanol, and dried in air. The attached F1BT2H was then desorbed from the TiO_2 surface by immersing the film in 5 mL of 0.01 M NaOH Ethanol/ H_2O

mixed solution (Ethanol:H₂O = 1:1 in volume ratio). The desorbed F1BT2H solution was diluted to 20 mL, and absorption spectrum of this diluted solution was measured. The amount of adsorbed F1BT2H molecules was calculated per cm² of projected TiO₂ area. The extinction coefficient of F1BT2H at the absorption maximum wavelength is 82000 M⁻¹cm⁻¹.⁷

Absorption spectra for the oxidized state of the P-F1BT2/TiO₂ were observed by the spectroelectrochemical method. The experiments were performed following the method described previously.⁸ The P-F1BT2/TiO₂ electrode was set to a three electrode cell with a quartz window, and placed in an absorption spectrometer (JASCO, V-670). Pt and Ag/AgCl electrodes were employed as counter and reference, respectively. Absorption spectra were observed after bias application into the electrode in 0.1 M LiClO₄ in PC for 5 min. The bias was applied from 0 V with +0.1 V steps following the measurement of the reference line after 15 min. stabilization at 0 V vs. Ag/AgCl.

Transient absorption studies were conducted on sub-microsecond to millisecond time scales with a Nd/YAG laser (Spectra Physics, Quanta-Ray GCR-11) pumped dye laser (Usho Optical Systems, DL-100, ~10 ns pulse duration) as a pump source, a 100 W tungsten lamp as a probe source, and a photodiode-based detection system (Costronics Electronics) with a TDS-2022 Tektronix oscilloscope.⁹ Transient data were obtained by employing a low excitation density ~30 μJ/cm² at 1 Hz with an excitation wavelength of 450 nm and 480 nm for the monomer and the conducting wire attached metal oxide films, respectively. This excitation density roughly corresponds to ~0.3 excited states created per TiO₂ nanoparticle.

3. Results

Absorption and emission spectra of F1BT2H in solution phase

Fig. S1 compares the absorption and emission spectra obtained for 10 μM F1BT2H ethanol solution. The broad absorption spectral shape with a peak wavelength of 395 nm is almost identical to the previously reported data for 2,7-Bis(2,2'-bithien-5-yl)-9,9'-dioctylfluorene.⁷ Belletete et al. reported that the ground state for this molecules possesses an antibonding character between neighboring rings, indicating that the ground state is flexible.

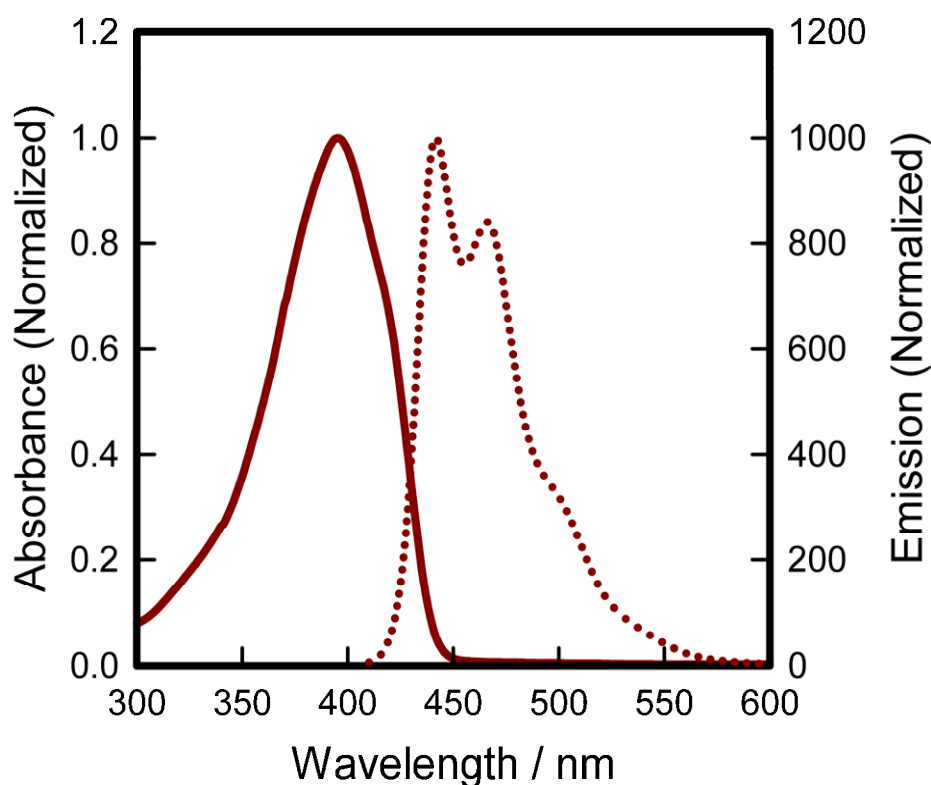


Fig. S1. Absorption (solid line) and emission (dotted line) spectra of 10 μM F1BT2H in ethanol. The excitation wavelength of the emission data is 400 nm.

In contrast, the emission spectrum exhibits at least three distinctive vibronic peaks with the highest peak of 442 nm, suggesting that the excited state possesses a narrower distribution of conformers.⁷

F1BT2H binding isotherm

Adsorption isotherm was measured by relating the amount of F1BT2H adsorbed on the TiO₂ surface to the solution equilibrium concentration. The results are shown in Fig. S2. Analysis of these data was conducted based on the Langmuir adsorption isotherm model, eq 1.

$$\frac{\Gamma}{\Gamma_0} = \theta = \frac{c_{eq} K_{ad}}{1 + c_{eq} K_{ad}} \quad (1)$$

where Γ is the adsorbed F1BT2H amount, Γ_0 is the maximum coverage amount, θ is the coverage, c_{eq} is the solution concentration at equilibrium, and K_{ad} is the adsorption constant. The estimated K_{ad} and Γ_0 by fitting the results with eq 1 are $7.0 \times 10^4 \text{ M}^{-1}$ and $9.3 \times 10^{-8} \text{ mol/cm}^2$, in fair agreement with the reported values for ruthenium dyes.¹⁰

The experimental results are clearly consistent with the Langmuir adsorption behavior. Following the BET measurement to estimate the TiO₂ film effective surface area, the coverage of F1BT2H on the TiO₂ surface for the film employed for the polymerization was evaluated to be approximately 50 %, assuming that one F1BT2H molecule occupies an area of 1.7 nm^2 (calculated from the intra-molecular distances). These data therefore suggest that F1BT2H is adsorbed on the monolayer level on the TiO₂ surface, and no sign of aggregation or stacking of F1BT2H molecules was appeared.

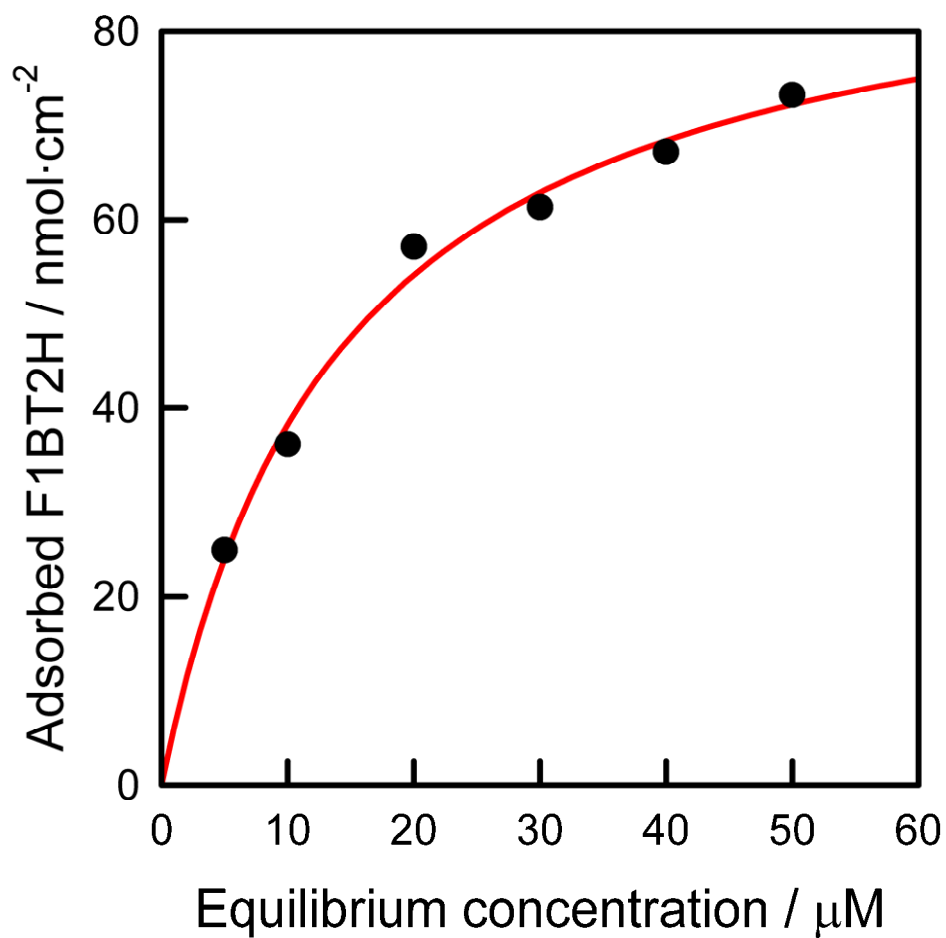


Fig. S2. Adsorption isotherm for F1BT2H attached TiO₂ films. A solid red line indicates a fit to a Langmuir adsorption isotherm, eq 1.

FT-IR spectra of the electrochemically polymerized F1BT2 on FTO and the P-F1BT2/TiO₂

Fig. S3 compares the FT-IR spectra of the P-F1BT2 prepared by two different methods, i) the electrochemically polymerized F1BT2 on FTO, and ii) P-F1BT2 on TiO₂ by the lateral charge transfer process under the positive bias application. The latter spectrum was obtained by subtracting the FT-IR spectrum of the TiO₂ alone from that of the P-F1BT2/TiO₂, owing to strong broad absorption by the TiO₂ at less than 800 cm⁻¹. The spectrum of the electrochemically polymerized F1BT2 on FTO exhibits a strong absorption band at approximately 800 cm⁻¹, being assigned to the C-H out-of-plane vibration, whilst no absorption band was observed at approximately 700 cm⁻¹. This observation clearly supports the polymer formation, i.e. 2,5-substituted thiophene.¹¹ In contrast, the spectrum of the P-F1BT2/TiO₂ shows both bands at approximately 700 and 800 cm⁻¹, suggesting existence of both the monomer and the conducting wire.

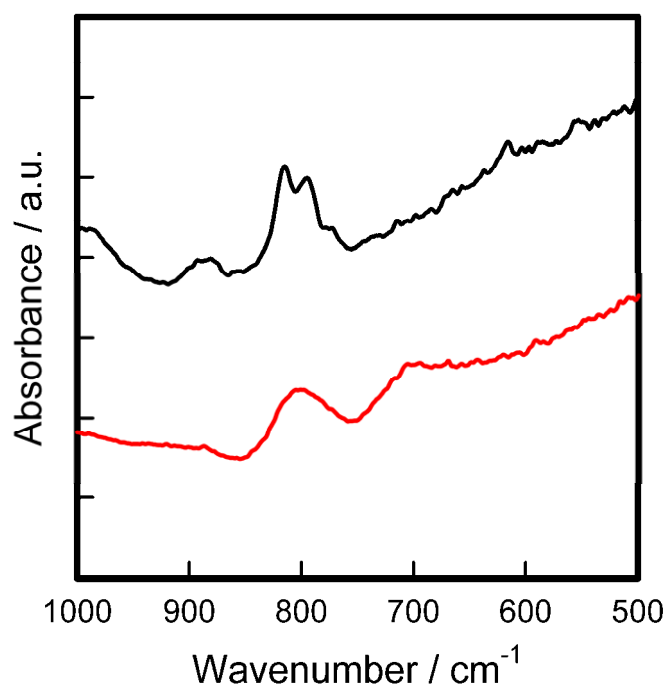


Fig. S3. FT-IR spectra of the electrochemically polymerized F1BT2 on FTO (black line) and the P-F1BT2/TiO₂ (red line).

Electrochemical formation of P-F1BT2 on Al₂O₃ nanocrystalline electrode

The conducting wire formation was performed on the surface of the Al₂O₃ nanocrystalline film by applying electrical bias of +1.0 V vs. Ag/AgCl to the F1BT2H attached electrode. The absorption spectrum of the polymer attached Al₂O₃ film, P-F1BT2/Al₂O₃, is compared with the monomer attached Al₂O₃ film, as shown in Fig. S4. By this electro-polymerization, the absorption onset of the P-F1BT2/Al₂O₃ is shifted to 550 nm from 465 nm. The formed polymer was insoluble in aqueous or non-aqueous solvents.

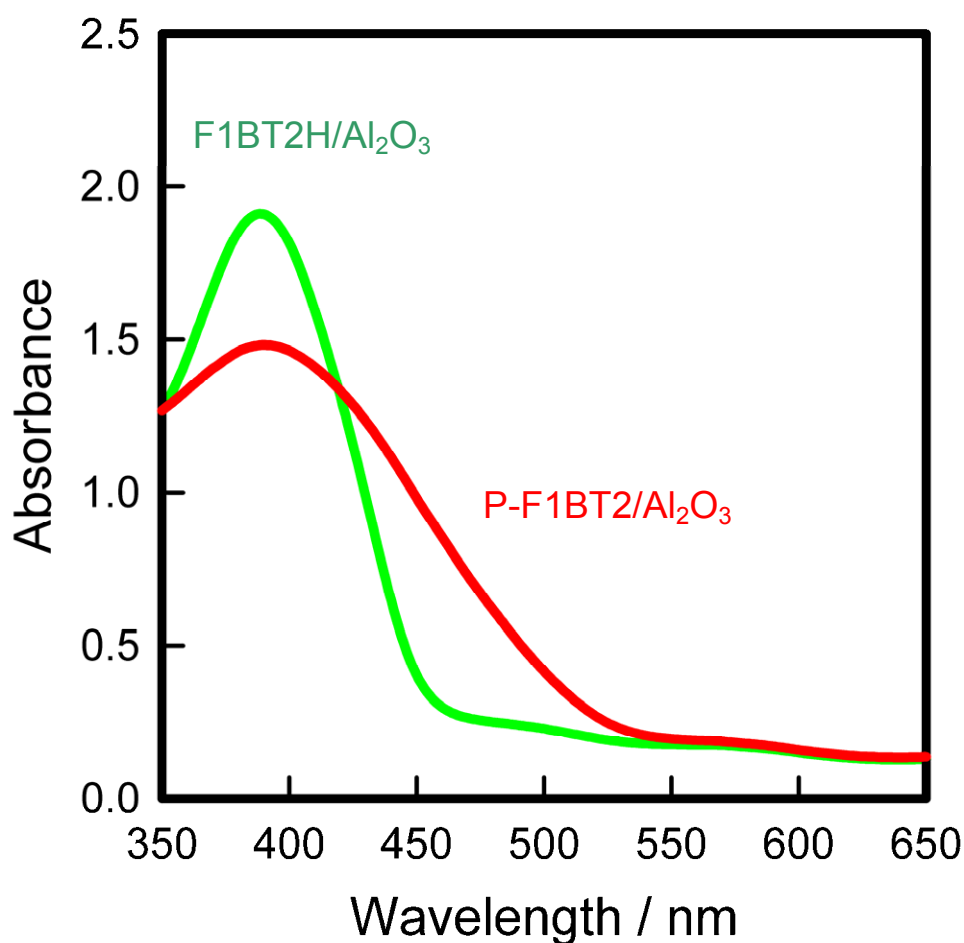


Fig. S4. Absorption spectra obtained for F1BT2H/Al₂O₃ (green line) and P-F1BT2/Al₂O₃ (red line).

Absorption difference spectra for P-F1BT2 oxidized states

The absorption spectra for the P-F1BT2/TiO₂ oxidized states were qualitatively generated spectroelectrochemically. Since the polymer wire can electrochemically be formed on the metal oxide surface sequentially, it is also possible to oxidize the P-F1BT2 by positive bias application. Fig. S5 shows the absorption spectral change of the P-F1BT2/TiO₂ by employing a three electrode cell with a quartz window, where the base line was observed at 0 V vs. Ag/AgCl. The bias application at >+0.6 V vs. Ag/AgCl generated the broad absorption with a peak at approximately 800 nm, probably attributed to the oxidized state absorption. Thus, this onset voltage corresponds to the P-F1BT2 HOMO level. Concomitant with this positive absorption, sharp bleach was also observed with a peak at 480 nm, probably attributable to the loss of the HOMO-LUMO transition.

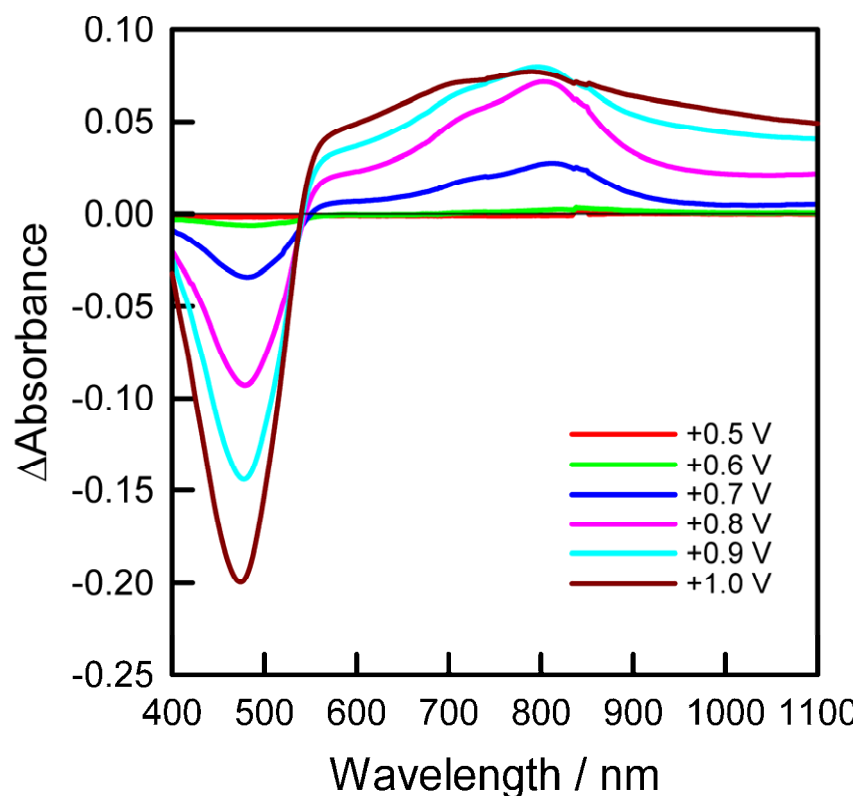


Fig. S5. Absorbance change of the P-F1BT2/TiO₂ under the electrical bias application (vs. Ag/AgCl).

Transient absorption decay kinetics

We have conducted transient absorption studies for control samples to support the data obtained for F1BT2H/TiO₂ and P-F1BT2/TiO₂. The charge recombination dynamics was investigated for F1BT2Br/TiO₂, namely, the monomer attached TiO₂ film. Fig. S6 shows a charge recombination profile observed at 660 nm following the 450 nm excitation. The charge recombination half lifetimes, $t_{50\%}$, is approximately 2 ms, being similar to that for F1BT2H/TiO₂. The decay kinetics was fitted with a stretched exponential function, $\Delta OD(t) = \Delta OD_0 \exp(-t/\tau)^\alpha$. The initial amplitude, ΔOD_0 , is normalized to unity, and the fitted stretch parameters, α , is 0.29, and the lifetimes, τ , is 7.0 ms. These data clearly support that the charge recombination behavior of the F1BT2Br/TiO₂ is almost identical to that of the F1BT2H/TiO₂.

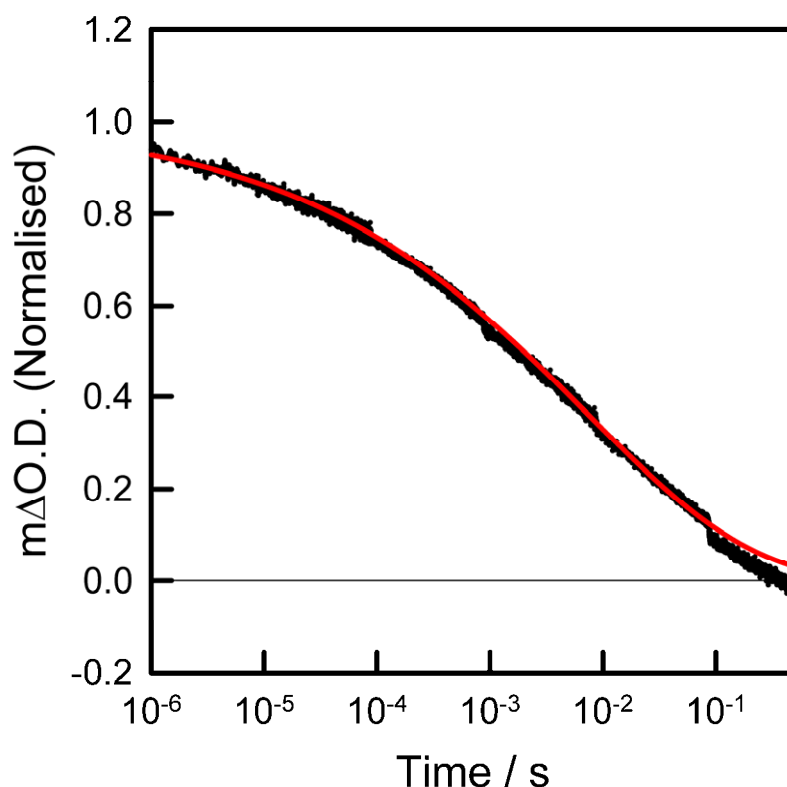


Fig. S6. Charge recombination kinetics of F1BT2Br/TiO₂ monitored at 660 nm with an excitation wavelength at 450 nm. A solid red line indicates a fit to a stretched exponential function, $\Delta OD(t) = \Delta OD_0 \exp(-t/\tau)^\alpha$.

The transient studies for the P-F1BT2/Al₂O₃ was also performed. Fig. S7 shows the transient absorption kinetics observed at 700 nm following the 450 nm excitation. The laser excitation energy density and the density of absorbed photons were adjusted to be identical to those observed for the P-F1BT2/TiO₂. As clearly seen in Fig. S7, the transient signal is small and the decay completes within 20 μ s. Since Al₂O₃ is known as an insulator, no electron acceptor state is available for the excited P-F1BT2. The transient signal therefore follows the tail of the P-F1BT2 excited state decay.

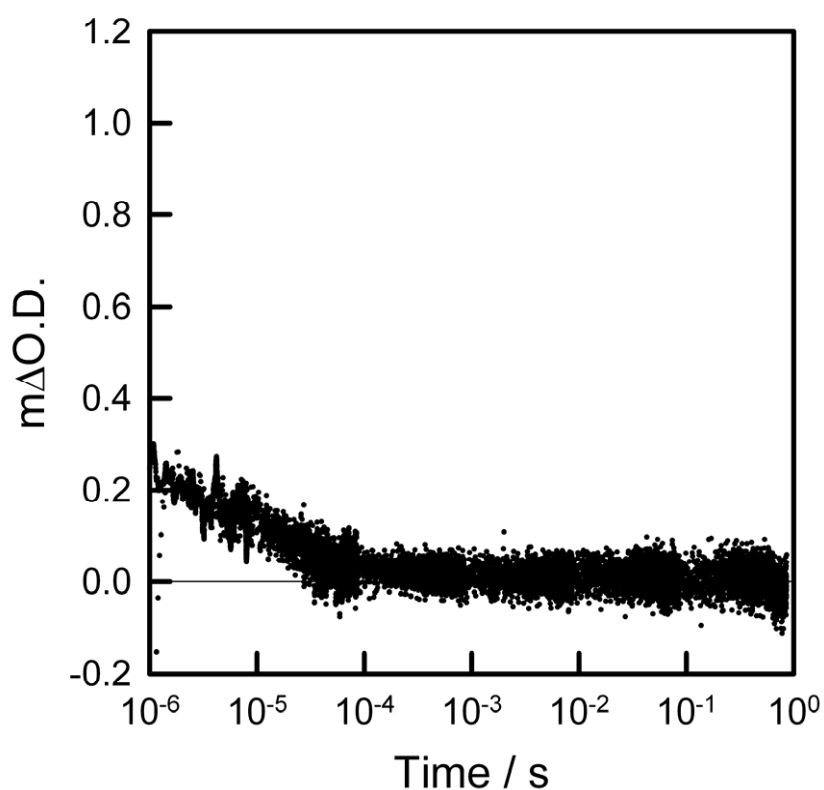


Fig. S7. Transient absorption kinetics for P-F1BT2/Al₂O₃, observed at 700 nm after the 450 nm excitation.

References

1. J. J. Michels, M. J. O'Connell, P. N. Taylor, J. S. Wilson, F. Cacialli and H. L. Anderson, *Chem.-Eur. J.*, 2003, **9**, 6167-6176.
2. Y. Otsuka, Y. Okamoto, H. Y. Akiyama, K. Umekita, Y. Tachibana and S. Kuwabata, *J. Phys. Chem. C*, 2008, **112**, 4767-4775.
3. Y. Wei, J. Tian, D. Glahn, B. Wang and D. Chu, *J. Phys. Chem.*, 1993, **97**, 12842-12847; R. J. Waltman, J. Bargon and A. F. Diaz, *J. Phys. Chem.*, 1983, **87**, 1459-1463.
4. A. Saeki, S. Seki, Y. Koizumi and S. Tagawa, *J. Photochem. Photobiol., A*, 2007, **186**, 158-165.
5. W. W. Scott and B. Bhushan, *Ultramicroscopy*, 2003, **97**, 151-169.
6. J. P. Cleveland, B. Anczykowski, A. E. Schmid and V. B. Elings, *Appl. Phys. Lett.*, 1998, **72**, 2613-2615; N. Zhao, G. A. Botton, S. Zhu, A. Duft, B. S. Ong, Y. Wu and P. Liu, *Macromolecules*, 2004, **37**, 8307-8312.
7. M. Belletete, J.-F. Morin, S. Beaupre, M. Ranger, M. Leclerc and G. Durocher, *Macromolecules*, 2001, **34**, 2288-2297.
8. G. Boschloo and D. Fitzmaurice, *J. Phys. Chem. B*, 1999, **103**, 7860-7868; R. van de Krol, A. Goossens and E. A. Meulenkaamp, *J. Appl. Phys.*, 2001, **90**, 2235-2242; R. L. Willis, C. Olson, B. O'Regan, T. Lutz, J. Nelson and J. R. Durrant, *J. Phys. Chem. B*, 2002, **106**, 7605-7613; S. A. Haque, Y. Tachibana, R. L. Willis, J. E. Moser, M. Grätzel, D. R. Klug and J. R. Durrant, *J. Phys. Chem. B*, 2000, **104**, 538-547.
9. Y. Tachibana, K. Umekita, Y. Otsuka and S. Kuwabata, *J. Phys. Chem. C*, 2009, **113**, 6852-6858.
10. K. Kils, E. I. Mayo, B. S. Brunschwig, H. B. Gray, N. S. Lewis and J. R. Winkler, *J. Phys. Chem. B*, 2004, **108**, 15640-15651; B. V. Bergeron, A. Marton, G. Oskam and G. J. Meyer, *J. Phys. Chem. B*, 2005, **109**, 937-943.
11. S. Hotta, W. Shimotsuma and M. Taketani, *Synth. Met.*, 1984, **10**, 85-94; Y. Furukawa, M. Akimoto and I. Harada, *Synth. Met.*, 1987, **18**, 151-156.